

# **Modelling of Axial Spring Stiffness in Active Vibration Controlled Drilling**

By

**Lim Peng Sheng**

**12635**

Dissertation submitted in partial fulfillment of  
the requirements for the  
Bachelor of Engineering (Hons)  
(Mechanical Engineering)

SEPTEMBER 2013

Universiti Teknologi PETRONAS  
Bandar Seri Iskandar  
31750 Tronoh  
Perak Darul Ridzuan

**CERTIFICATION OF APPROVAL**

**Modelling of Axial Spring Stiffness in  
Active Vibration Controlled Drilling**

by

Lim Peng Sheng

A project dissertation submitted to the  
Mechanical Engineering Programme  
Universiti Teknologi PETRONAS  
in partial fulfilment of the requirement for the  
BACHELOR OF ENGINEERING (Hons)  
(MECHANICAL ENGINEERING)

Approved by,

---

(Dr. Setyamartana Parman)

UNIVERSITI TEKNOLOGI PETRONAS  
TRONOH, PERAK  
SEPTEMBER 2013

**CERTIFICATION OF ORIGINALITY**

This is to certify that I am responsible for the work submitted in this project, that the original work is my own except as specified in the references and acknowledgements, and that the original work contained herein have not been undertaken or done by unspecified sources or persons.

---

LIM PENG SHENG

## **ABSTRACT**

During drilling process, substantial amount of vibration and shock are induced to the drill string. Active vibration controlled drilling is introduced to reduce the vibration and increase the efficiency of drilling process. In this system, two main components that determine the damping stiffness are MR damper and spring assembly. Performance of vibration damping system is depending on the viscosity of MR fluid in the damper and spring constant of spring assembly. One of the key issues that are unclear from the design is the correlation between the axial spring stiffness configuration and the damping force which needs to be tuned actively. There has been lack of studies on how the viscosity of MR fluid on the active vibration damper affects the damping stiffness of the whole system. The first objective of the project is to investigate the relationship between the damping coefficient and power input to the system. Second objective is to develop the correlation between the viscosity of magnetorheological (MR) fluid and axial spring stiffness. To achieve the objectives, model of vibration damping system is created using MATLAB Simulink. The model is built with reference of experimental data conducted by APS Technology. Inputs of the simulation such as force exerted, mass of mandrel, spring constant and step time are based on the experimental data and can be adjusted to suit different experiments. By having the model, behavior of the system can be studied and analyzed. From the simulation, it is also observed that the relationship between damping coefficient and power input of the system is linear.

**Keywords:** Magnetorheological Fluid; Magnetorheological Damper; Damping Coefficient; MATLAB Simulink

# Contents

CHAPTER 1: INTRODUCTION .....	1
1.1 Project Background.....	1
1.2 Problem Statement .....	3
1.3 Objectives.....	3
1.4 Scope of Study.....	3
CHAPTER 2: LITERATURE REVIEW.....	4
CHAPTER 3: METHODOLOGY .....	10
3.1 Research Methodology.....	10
3.2 Project Activities .....	11
3.3 Gantt Chart.....	12
CHAPTER 4: RESULT & DISCUSSION .....	13
4.1 Experiment Result.....	13
4.2 MATLAB Simscape Simulation .....	15
4.3 MATLAB Simulink Simulation .....	16
4.3 Frictional Force of the System .....	18
4.4 Damping Coefficient of the System .....	19
4.5 Simulink Simulation Result .....	20
4.6 Time Shift.....	23
CHAPTER 5: CONCLUSION.....	24
REFERENCE.....	25
APPENDIX.....	27

## Table of Figures

Figure 1.1: Three forms of drill string vibrations.....	1
Figure 1.2: Vibration damping system.....	2
Figure 2.1: MR fluid behavior.....	4
Figure 2.2: MR fluid damper.....	5
Figure 2.3: Belleville spring and example of 2-1-3-2 spring stack arrangement....	6
Figure 2.4: Shear stress against shear rate in Bingham model.....	7
Figure 3.1: Research methodology flowchart.....	10
Figure 3.2: Project activities flowchart.....	11
Figure 4.1: Experiment set up conducted by APS Technology.....	13
Figure 4.2: Experimental data for power 33% and 70% .....	14
Figure 4.3: Force spring mass system.....	15
Figure 4.4: Simulation of force spring mass system using Simscape.....	16
Figure 4.5: Simulation of force spring mass system using Simulink.....	17
Figure 4.6: Subsystem of frictional 1 force.....	17
Figure 4.7: Subsystem of damping coefficient.....	17
Figure 4.8: Graph of damping coefficient against power.....	19
Figure 4.9: Graph of total force against time.....	20
Figure 4.10: Displacement graph of power 33%.....	21
Figure 4.11: Displacement graph of power 70%.....	22

## **Table of Tables**

Table 1: Gantt chart.....	12
Table 2: Experimental and simulation result for power 33%.....	27
Table 3: Experimental and simulation result for power 70%.....	29

## CHAPTER 1: INTRODUCTION

### 1.1 Project Background

Underground drilling, such as gas, oil or geothermal drilling, generally involves drilling a bore through a formation deep in earth. Such bore are form by drill string which consists of several drill pipes, drill collars, and stabilizes and connection (crossover sub). During drilling process, substantial amount of vibration and shock are induced into the drill string. Drill string is under some heavy and complex dynamics loadings, caused by different sources such as rotation of drill bit, the motor used to rotate the drill string, pumping drilling mud, and misalignment of drill string. By producing different state of stresses, these loads may result in excess vibrations and lead to failure of the drilling tools. Three forms of vibrations have been identified for drill string, namely are axial, torsional and lateral vibrations.

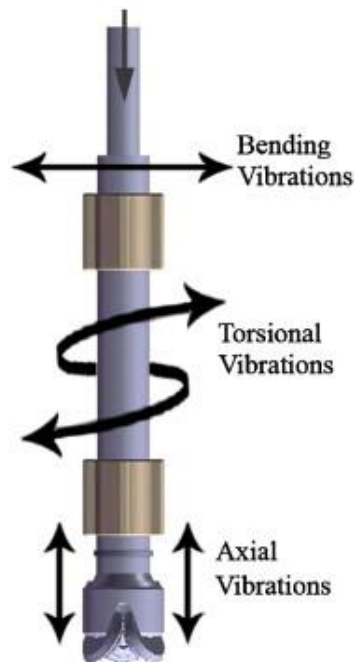


Figure 1.1: Three forms of drill string vibrations (Spanos *et al*, 2003)

Bending vibrations which are known as lateral vibrations can cause the bending and whirl of drill string during the drill process. It is the most destructive type of vibration and can create large shock as the bottom hole assembly impacts the wellbore wall. Torsional vibrations can cause irregular downhole rotation and stick slip effect. They can damage the drill bits and caused fatigue on drill collar connections. Axial vibrations can cause bit bounce which may damage bit cutters and bearings.

Active vibration control drilling is introduced to increase the efficiency of drilling and decrease the premature failure during drilling process. As shown in Figure 2, three main parts of vibration damping system are magnetorheological (MR) fluid valve assembly (18) , spring assembly (16) and torsional bearing assembly (22).

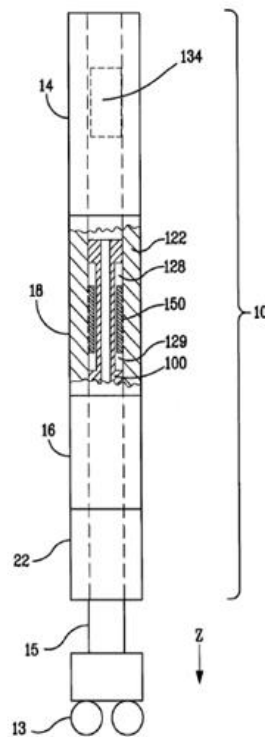


Figure 1.2: Vibration damping system (Wassell *et al*, 2012)

## **1.2 Problem Statement**

In active vibration control drilling, two main components that determine the damping stiffness are MR damper and spring assembly. Performance of vibration damping system is depending on the viscosity of MR fluid in the damper and spring constant of spring assembly.

One of the key issues that are unclear from the design is the correlation between the axial spring stiffness configuration and the damping force which needs to be tuned actively. There has been lack of studies on how the viscosity of MR fluid on the active vibration damper affects the damping stiffness of the whole system.

## **1.3 Objectives**

The research objectives can be summarized as follow:

- a) To investigate the relationship between the power input of the system and damping coefficient of the damper.

## **1.4 Scope of Study**

The main focus of the research is to develop the relationship between the viscosity of magnetorheological (MR) fluid and the damping force of the drill string with the scope of:

- a) MR damper studied having fixed gap height, piston radius and coil width.
- b) Effect of axial vibration on MR damper, spring and vibration system.

## CHAPTER 2: LITERATURE REVIEW

Main components in active vibration control drilling are magnetorheological (MR) fluid, MR damper and Belleville spring. Wassell *et al* (2012) stated that MR fluid is suspension of magnetically polarizable micron-size particles dispersed in carrier liquid such as silicon oil, mineral oil or water. In the normal conditions, MR fluid has the flow characteristic of conventional oil. In the presence of magnetic field, the particles suspended in the carrier fluid become polarized. The polarization causes the particles to become organized in chains within the carrier fluid. Flow viscosity and fluid shear strength increases as the particle chains in MR fluid increases. Upon removal of the magnetic field, the particles return to an unorganized state. Thus, by controlling the magnetic field, it allows the strength and flow resistance of MR fluid to alter rapidly.

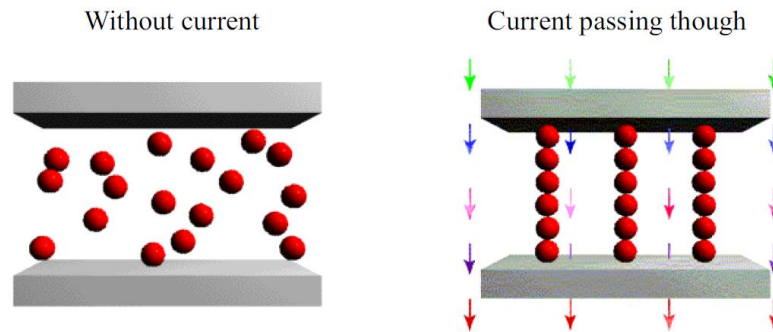


Figure 2.1: MR fluid behavior (Wassell *et al*, 2012)

Walid H.E. (2002) stated that in MR dampers are semi-active devices that contain MR fluid. Presence of magnetic field results in changes of viscosity of the MR fluid, causing a pressure differential for the flow of fluid in the orifice volume. The pressure differential is directly proportional to the force required to move the damper rod. As such, the damping characteristic of the MR damper is a function of the electrical current flowing into the electromagnet. This relationship allows the damping of an MR damper to be easily controlled in real time.

Kciuk *et al* (2011) reported that ability of MR fluid changes from liquid to semi-solid state in few milliseconds result is an infinitely variable, controllable damper capable of large damping forces. MR dampers offer an attractive solution to energy absorption in mechanical systems and structures and can be considered as “fail-safe” devices.

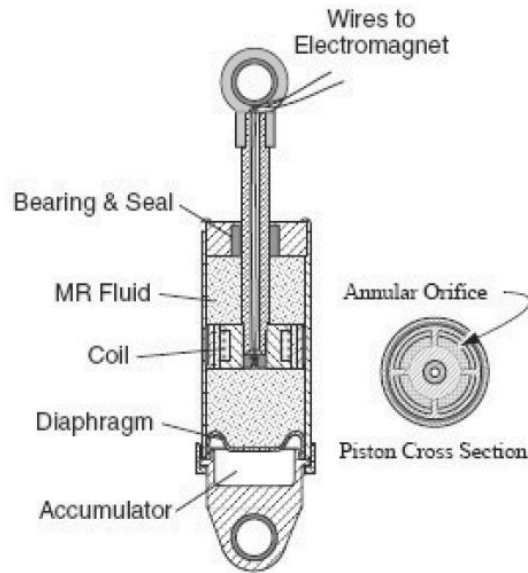


Figure 2.2: MR fluid damper (Kciuk *et al*, 2011)

In active vibration control drilling, Belleville spring is connected at the bottom of MR to form active vibration damper. Dubey *et al* (2012) reported that stress and deflection of Belleville spring is affected by the ratio of height to thickness ( $h/t$ ) and outer diameter to inner diameter of spring ( $D/d$ ). The spring force of a single spring can be calculated by using the formula as shown:

$$F = \frac{4E\delta}{1-\mu^2} \times M \times D^2 \times \left[ (h-t) \left( h - \frac{\delta}{2} \right) t + t^3 \right] \quad (2.1)$$

where

$E$  = Spring modulus of elasticity

$\mu$  = Poisson's ratio

- $\delta$  = Deflection of a single spring
- $M$  = Calculation coefficients
- $t$  = Spring material thickness
- $h$  = Unloaded spring height
- $D$  = Outer diameter of spring
- $d$  = Inner diameter of spring

Stacking formula of the Belleville spring is as shown:

$$K = \frac{k}{\sum_{i=1}^g \frac{1}{n_i}} \quad (2.2)$$

where

- $K$  = Spring constant of spring stack
- $k$  = Spring constant of single spring
- $n_i$  = Number of spring in the  $i^{\text{th}}$  group
- $g$  = Number of groups.

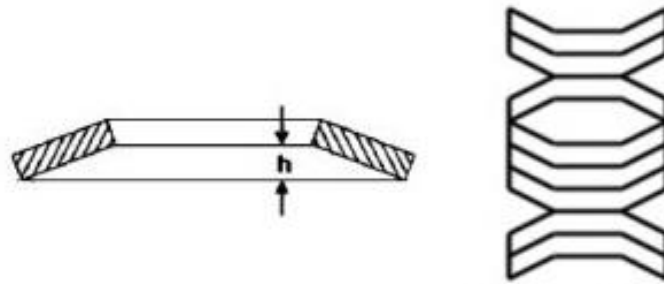


Figure 2.3: Belleville spring and example of 2-1-3-2 spring stack arrangement (Fromm *et al*, 2003)

Behavior of MR fluid can be categorized into Bingham model and Carreau model. Ashfak *et al* (2011) and Walid (2002) reported MR fluid behaves as a Bingham plastic with variable yield strength when activated. The shear stress associated with the flow of MR fluid can be predicted by the Bingham equation:

$$\tau = \tau_y(B) + \eta\gamma, \tau > \tau_y \quad (2.3)$$

where

$\tau_y$  = Shear stress

$\eta$  = Plastic viscosity independent on magnetic field

$\gamma$  = Shear rate.

Parlak *et al* (2012) stated that using ANSYS to achieve FEM analysis of magnetic field and fluid flow simultaneously based on Bingham plastic model.

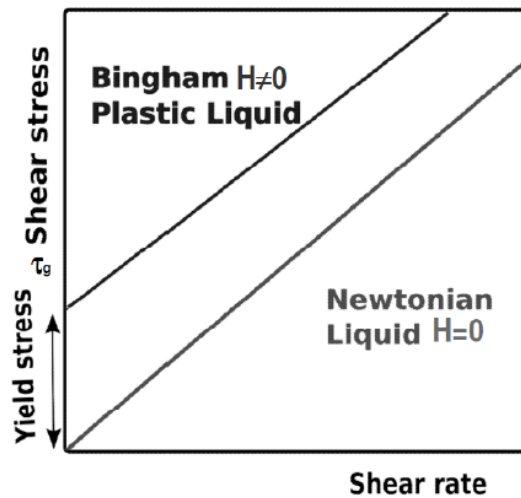


Figure 2.4: Shear stress against shear rate in Bingham model (Bajkowski *et al*, 2012)

On the other hand, Allotta *et al* stated that Bingham model is difficult to achieve from computational point, thus Carreau Model equation is selected for smoother analysis:

$$\eta = \eta_{\infty} + (\eta_0 - \eta_{\infty})[1 + (\lambda y)^2]^{\frac{n-1}{2}} \quad (2.4)$$

where

- $\eta$  = Value of viscosity
- $\eta_0$  = Viscosity for shear rate equal to zero
- $\eta_{\infty}$  = Viscosity for high shear rate
- $\lambda$  = Carreau constant
- $n$  = Carreau constant
- $y$  = Shear rate

The main behavior of a MR damper is damping force which can be calculated by multiply the pressure drop with the piston cross section area of the damper according to Ashfak *et al* (2011). Meanwhile, Allotta *et al* stated that it is possible to compute the total force of damper by summing up the force in the fluid due to the magnetic field ( $F_{\tau}$ ) and the force in the fluid due to the fluid viscosity ( $F_{\eta}$ ) .

$$F = F_{\tau} + F_{\eta} \quad (2.5)$$

$$F_{\tau} = \frac{c\tau_0 L_{pc} A_p}{g} \quad (2.6)$$

$$F_{\eta} = \frac{12Q\eta L_p A_p}{\pi g D_p} \quad (2.7)$$

where:

- $c$  = Parameter function of  $F_{\tau}/F_{\eta}$
- $\tau_0$  = Yield stress due to the applied magnetic field
- $L_{pc}$  = Total length of the polar expansion

- $A_p$  = Piston area
- $g$  = Height of fluid duct
- $\eta$  = Kinematic viscosity
- $Q$  = Volumetric flow rate
- $L_p$  = Piston length
- $D_p$  = Piston diameter

Bajkpwski (2012) reported that further simplifications which were crucial for the computation of the damper's performance are:

- a) The damping force acts liner.
- b) The flow gap is formed by stationary wall.
- c) Height of the gap is much smaller than its length and the width, therefore the flow is considered as a flow between parallel plates.
- d) Stress value is constant along the gaps, it depends only on the value of the magnetic flux in the gap.

## CHAPTER 3: METHODOLOGY

### 3.1 Research Methodology

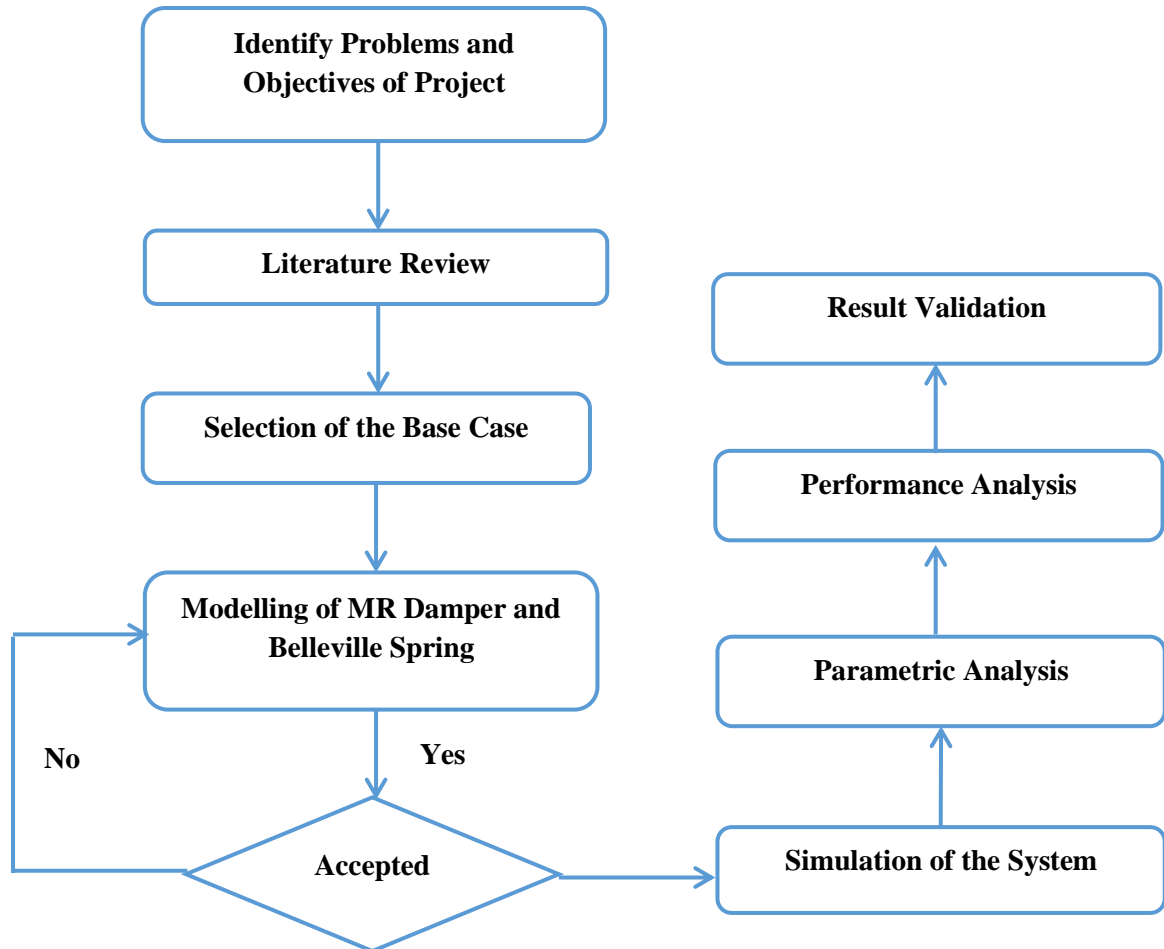


Figure 3.1: Research methodology flowchart

Firstly, problem statement and objectives of the project were identified. Literature review was done and suitable software is selected to suit the objectives. In this project, MATLAB Simulink is used to simulate the vibration damping system. MATLAB enable mandrel mass, spring constant and damping coefficient of the system to be controlled to meet the optimum operating range. Results from the simulation will be studied and analyzed to investigate the relationship between the damping coefficient and damping force of the system.

### 3.2 Project Activities

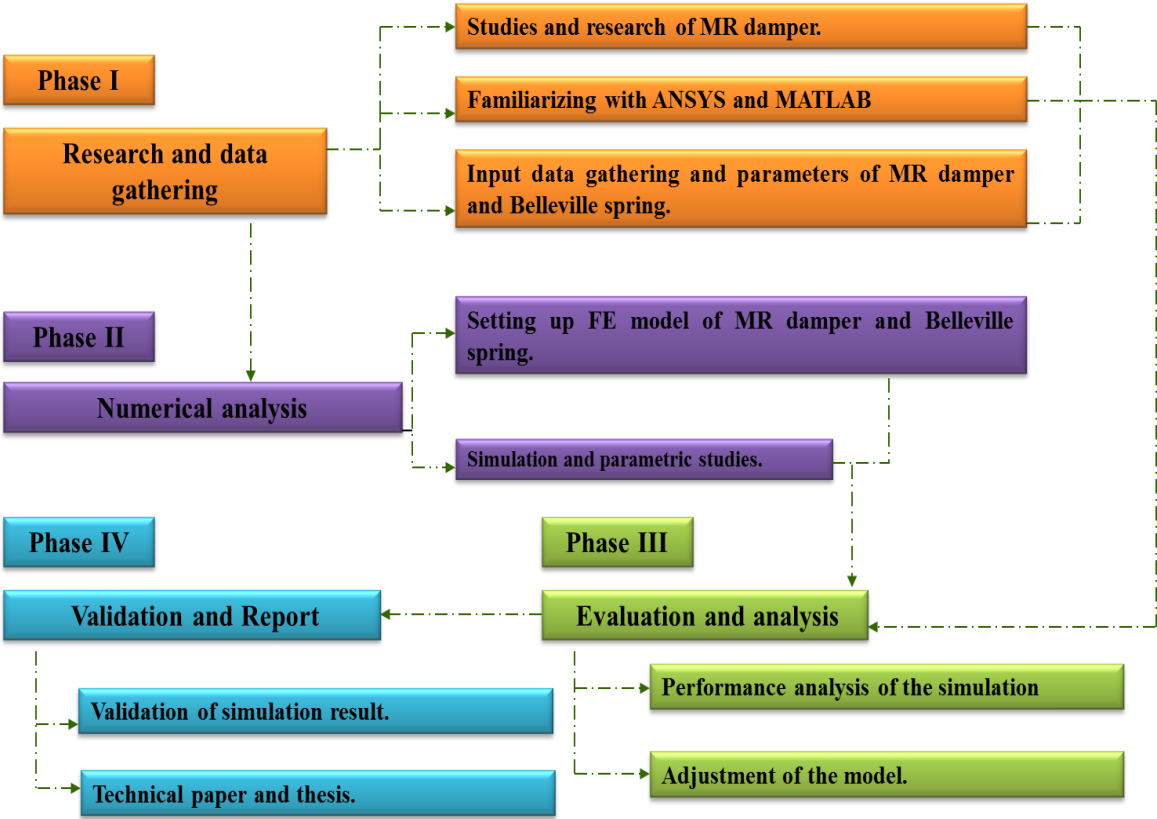


Figure 3.2: Project activities flowchart

The project activities are divided into 4 phases. The project is currently in phase II which is modeling and simulating the vibration damping system.

### 3.3 Gantt Chart

Table 1: Gantt chart

	FYP 1							FYP 2						
Research Activities	2	4	6	8	10	12	14	16	18	20	22	24	26	28
Background Studies	█													
Research and Data Gathering		█	█	█										
Selection of Base Case				█	█									
Modelling of MR Damper and Belleville Spring						█	●							
Simulation of the System								█	●					
Parametric Studies										█	█			
Performance Analysis											█	●		
Validation of Result												█		
Submission of Thesis													█	█

● Key Milestones

## CHAPTER 4: RESULT & DISCUSSION

### 4.1 Experiment Result

Experiments are done by APS Technology in Connecticut, USA as shown in Figure 4.1. 20 000 experimental data points are produced with 1 millisecond interval for each point. Averaging of data points are done to create average curve of the experiment result. Every data point with 0.1s interval is selected and produced the graph as shown in Figure 4.1. Total of 41 data point are selected for each curve. From Figure 4.2, it can be observed that the displacement of power 70% is smaller than the power 33%. Both curves are having same initial position which is 3in and similar trend throughout the 4s. Displacement dropped drastically in the 1<sup>st</sup> second. Next, displacement is fluctuating between 0.2in to 0.9in from 1st seconds to 4<sup>th</sup> second. However, displacement does not reach zero due to the frictional force.

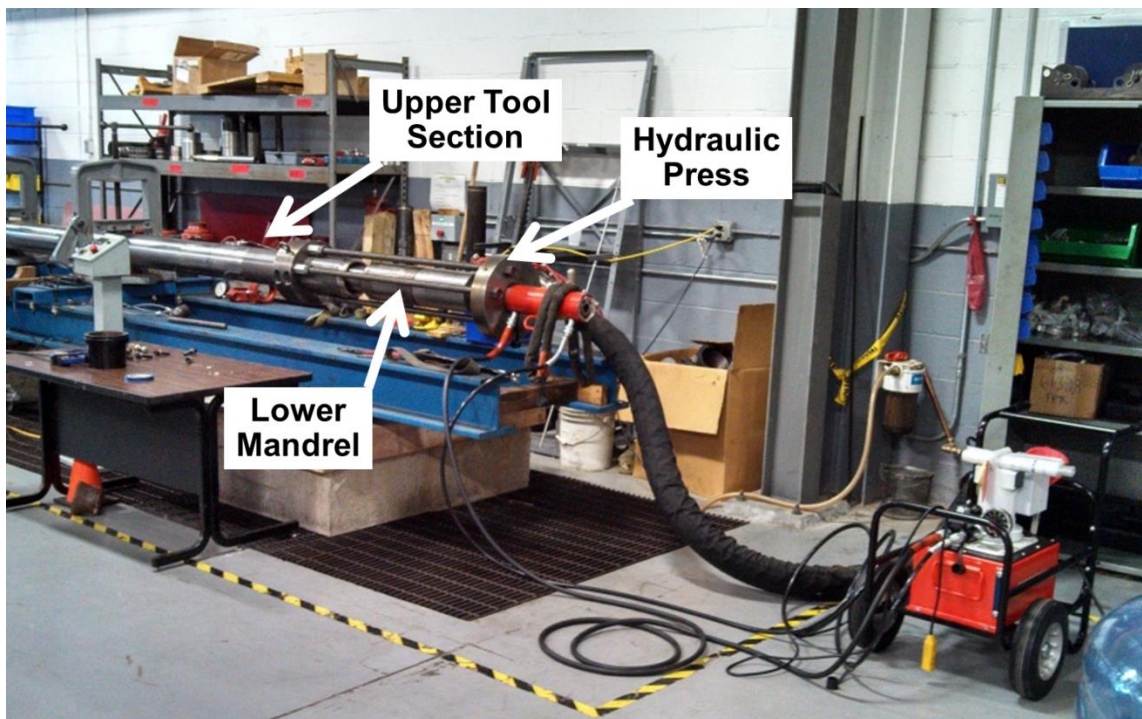


Figure 4.1: Experiment set up conducted by APS Technology

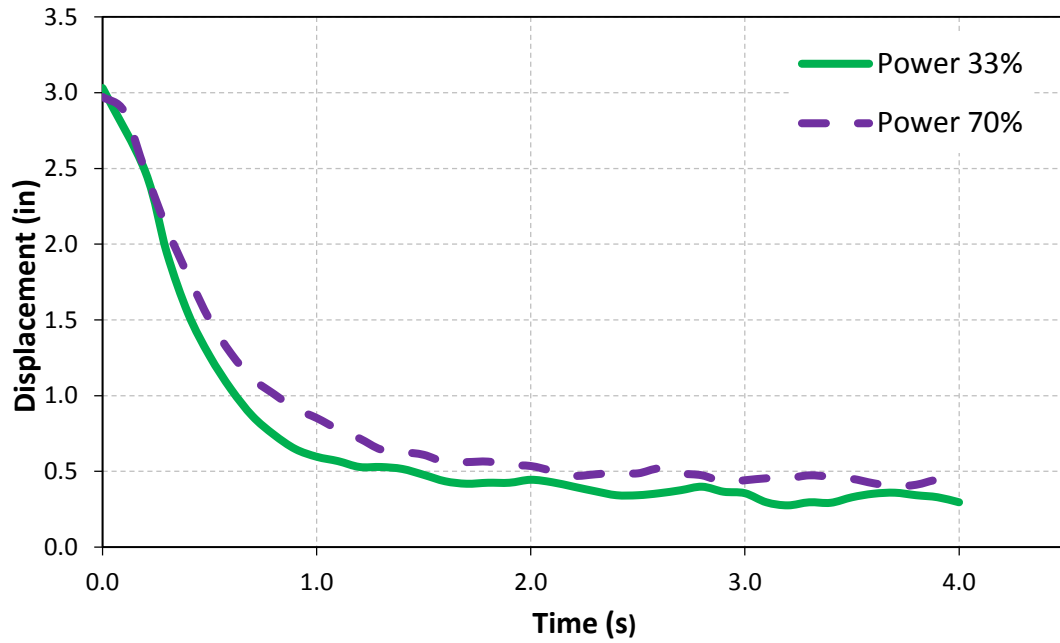


Figure 4.2: Experimental data for Power 33% and 70%

## 4.2 MATLAB Simscape Simulation

In this project, simulation model of vibration controlled drilling system is created to represent the experiment set up of APS Technology. This system can be simplified to force spring mass damper system as shown in Figure 4.3 where  $F$  is the axial force applied to the mandrel and  $M$  is the mass of mandrel.

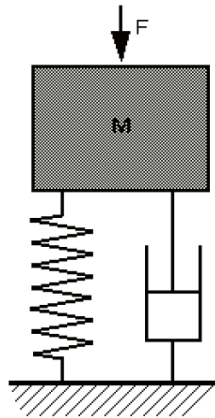


Figure 4.3: Force spring mass system

In order to predict the behavior and displacement of the force spring mass system, model is constructed by using MATLAB Simscape. As shown in Figure 4.4, model is constructed by connecting the block diagram of force source and mass to the translational spring and translational damper. Next, the system is connected to translational motion sensor to record the displacement and velocity data. Various inputs and block parameters of the model such as force profile, spring constant and damper coefficient can be adjusted accordingly to achieve the best result.

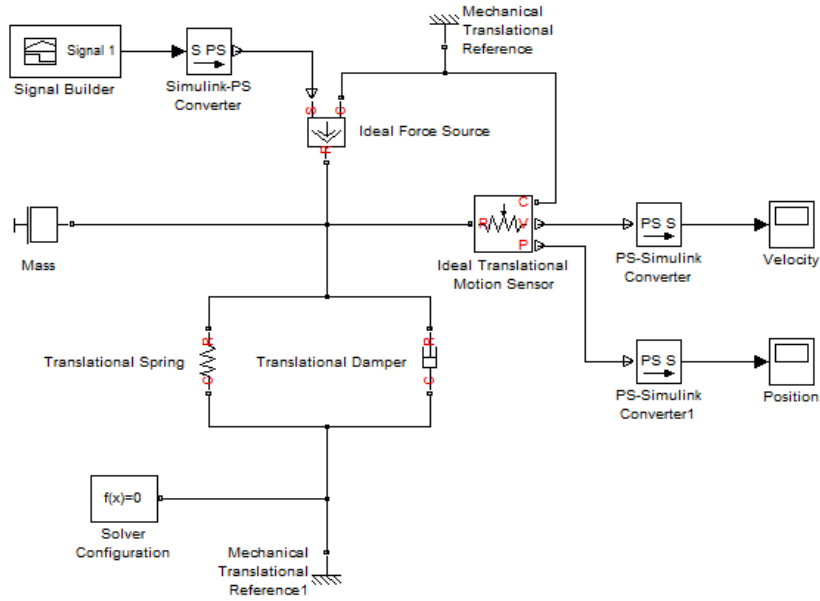


Figure 4.4: Simulation of force spring mass system using Simscape

In Simscape, model is constructed by blocks representing physical component and physical relationship between them. In Simscape, the connections represent physical connections between the components and they can have units. Available blocks in Simscape are not sufficient to represent the model and making it harder to alter the model. Moreover, variables input of Simscape is less user friendly. MATLAB Simulink is selected to model the vibration controlled drilling system.

### 4.3 MATLAB Simulink Simulation

Simulink is a block-diagram-oriented computer package to simulate dynamic system. It can also interface with the MATLAB environment for maximum flexibility. Mathematical model can be created by using blocks from Simulink blocks library. In addition, there are numerous ways to add custom blocks and functionality into the system. Vibration controlled drilling system can be constructed by using the formula

$$F = m\ddot{x} + c\dot{x} + kx \quad (4.1)$$

$$\ddot{x} = \frac{1}{m}(F - c\dot{x} - kx) \quad (4.2)$$

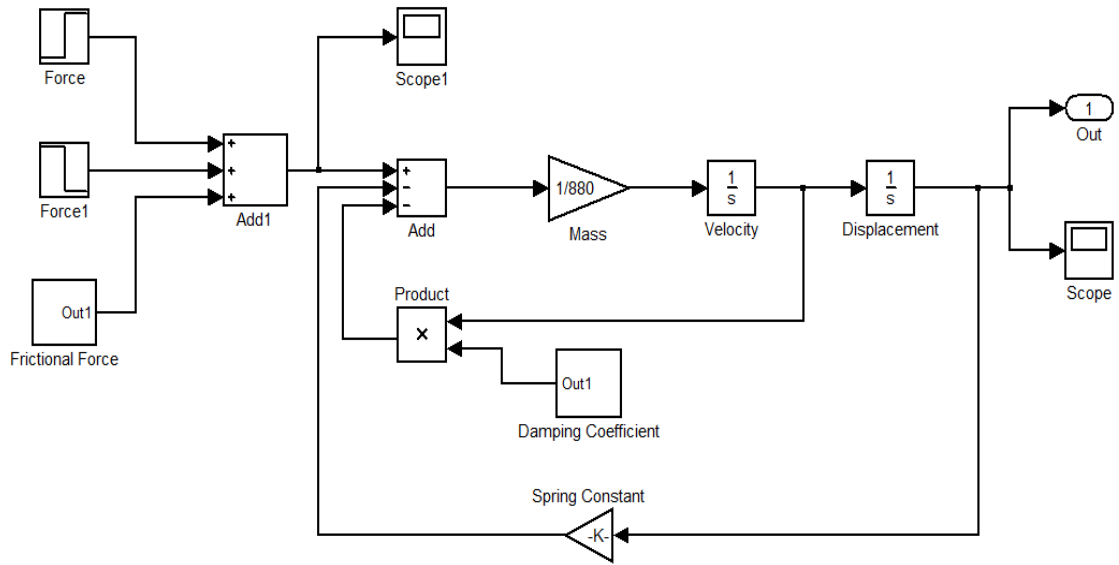


Figure 4.5: Simulation of force spring mass system using Simulink

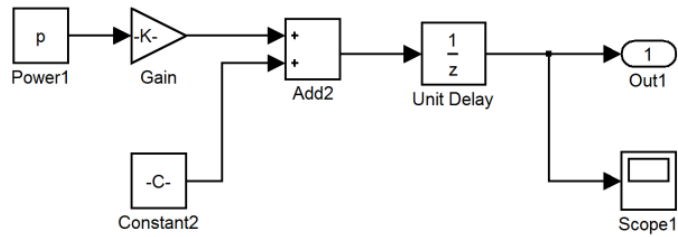


Figure 4.6: Subsystem of frictional force

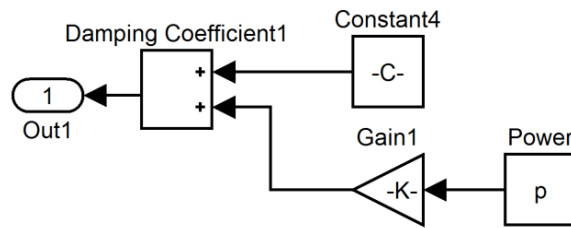


Figure 4.7: Subsystem of damping coefficient

From Figure 4.5 above, it can be seen that the Simulink model is constructed based on equation 4.2. First the force applied on the mandrel and frictional force are added into the system. Next, loop of damping coefficient is created by multiplying with mass and velocity. Spring constant loop is created by the product of displacement and mass. Scope block is used to display the input with respect to the simulation time. Out block is used to extract the result data for further usage. Subsystem of frictional force and subsystem of damping coefficient are included in the simulation to insert liner equations. Besides that, Simulink is more user friendly compare to Simscape which power input of the system can be defined easily by inserting the value in the command window.

### 4.3 Frictional Force of the System

Frictional force generated during the shearing of MR fluid. Inter-particles friction generated when two or more particles pile up along the field, frictional stress occurred in opposite direction of shear stress.

Frictional force is included in this system and it is depends on the type of the used sealing, construction material, piston velocity, duration of piston rest time and other. Frictional force occurs when the mandrel is release with the value of 4141lbf for power 33% and 6626lbf for power 70%. To calculate the equation of frictional force, first the slope of curve is determine by using equation  $y = mx + c$ ,

$$m = \frac{(6626 - 4141)}{(0.7 - 0.33)} = 6716.22$$

$$c = 6626 - 6716.22(0.7) = 1924.65$$

Thus frictional force is constructed as a subsystem as shown in Figure 4.6 with the equation of

$$F_r = 6716.22P + 1924.65 \tag{4.3}$$

Where P = percentage of power/100

#### 4.4 Damping Coefficient of the System

By using the trial and error method, damping coefficients of the system are identified as 8250lb·s/in for power 33% and 9100lb·s/in for power 70%. To determine the equation of damping coefficient, the calculation is similar as frictional force where slope is determined using the liner equation  $y = mx + c$ ,

$$m = \frac{(9100 - 8250)}{(0.7 - 0.33)} = 2297.30$$

$$c = 9100 - 2297.30(0.7) = 7491.90$$

Thus damping coefficient is constructed as a subsystem as shown in Figure 4.7 with the equation of

$$D = 2297.3P + 7491.9 \quad (4.4)$$

Where P = percentage of power/100

From the equation 4.8, graph of damping coefficient against power is constructed as shown in figure 4.6. From the graph, it can be seen that relationship between damping coefficient and power is linear.

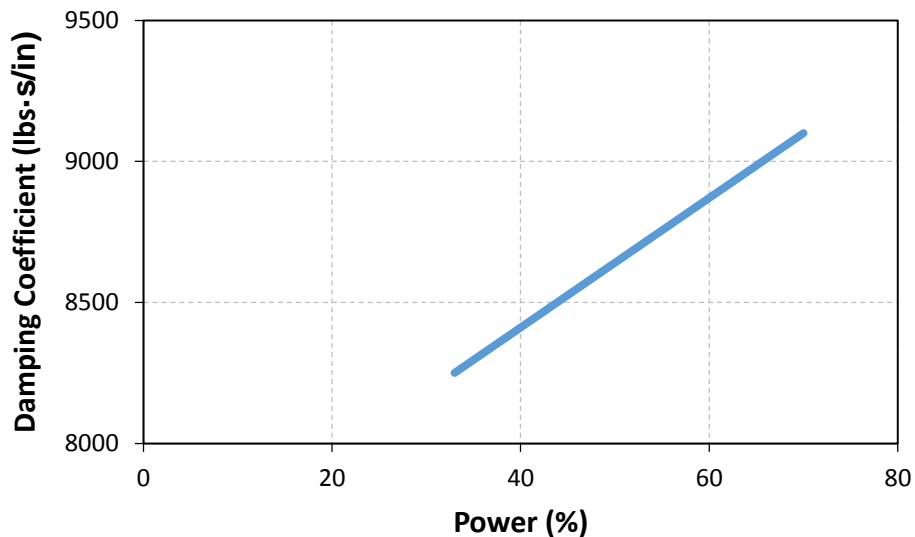


Figure 4.8: Graph of damping coefficient against power

#### 4.5 Simulink Simulation Result

To simulate the simulation, input data used for the experiments are defined in the model. Initial applied force on mandrel is 49 000lbf, mass of the mandrel is 880lb and spring constant of the system is 16565lbf/in. Percentage of power is defined in the command windows of MATLAB prior running the simulation.

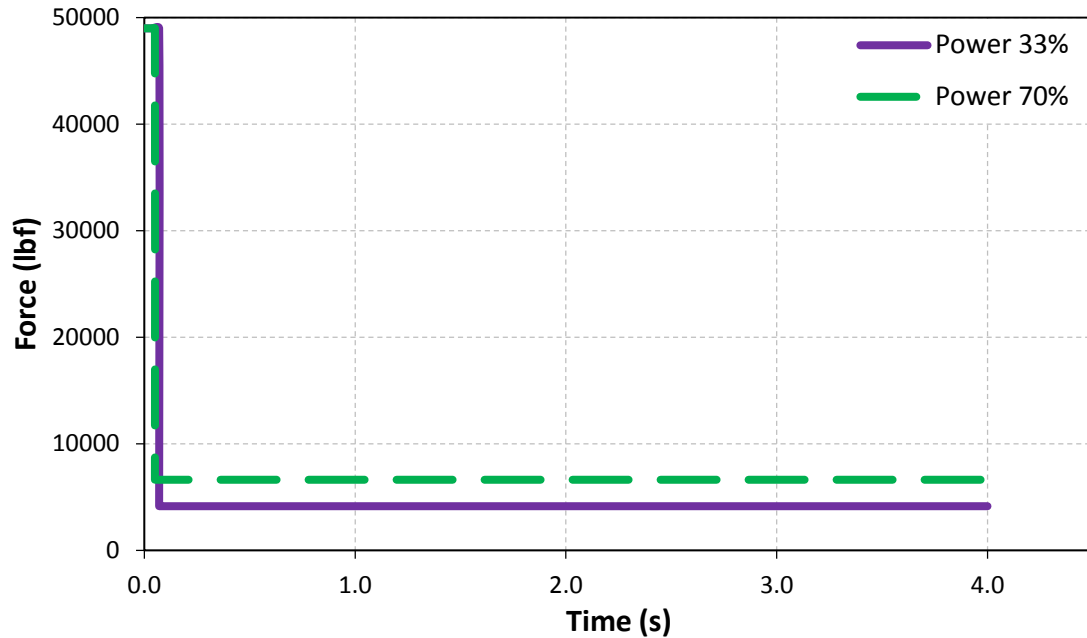


Figure 4.9: Graph of total force against time

Initial displacement of the system is 3in while step time of simulation is 4s. First 4s of the simulation is most crucial part where the maximum change of displacement occurred. Mandrel is released at 0.07s for power 33% and 0.05s for power 70%. Frictional force occurs once the mandrel is released. Thus frictional force of power 33% starts at 0.07s and 0.05s for power 70%. Force profiles of both systems are as shown in Figure 4.9.

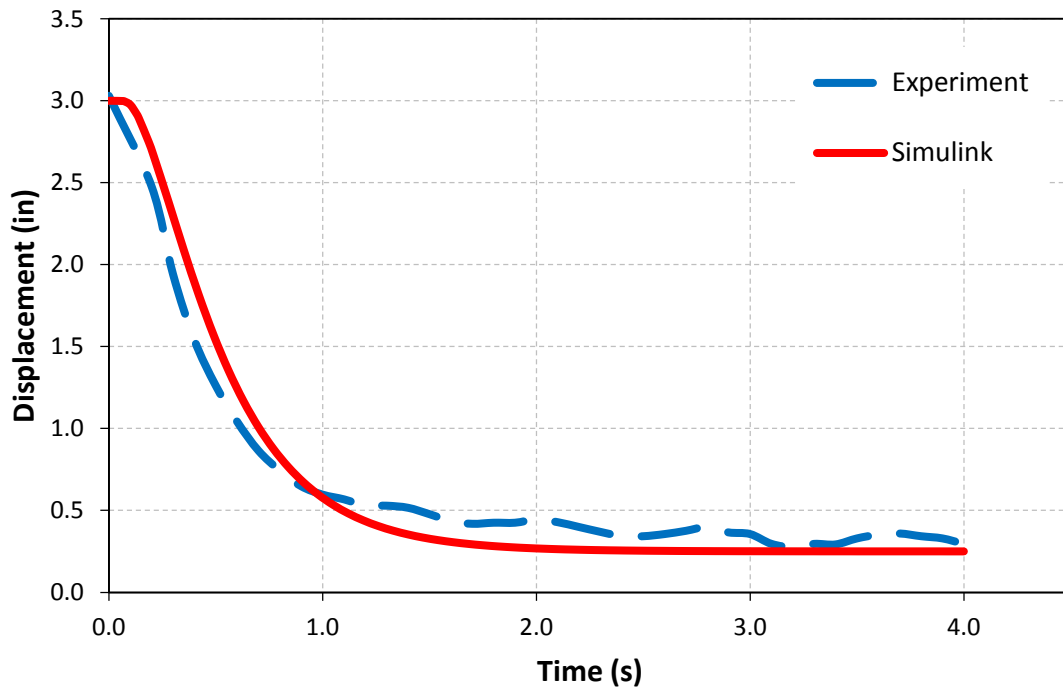


Figure 4.10: Displacement graph of power 33%

Figure 4.10 shows the comparison of MATLAB Simulink simulation result and APS Technology experimental result for system with power 33%. Trend of simulation curve and experiment curve are similar. The gradient of both curves are similar although the mandrel is released earlier in the experiment. Simulation curve is constant starting from 2s, however it does not drop to zero due to the frictional force in the mandrel. From the experimental curve provided by APS Technology, it can be seen that displacement is fluctuating form 2s to 4s. This phenomenon could be caused by noise and error when conducting the experiment. However, the deviation is small comparing to simulation result thus making it within acceptable range of value.

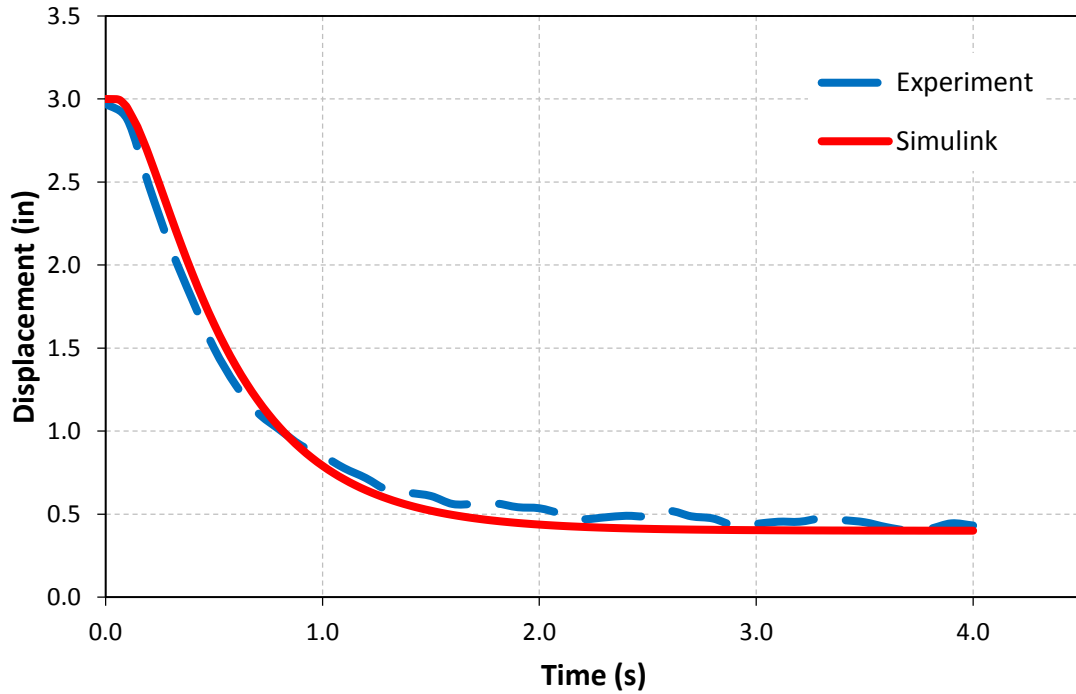


Figure 4.11: Displacement graph of power 70%

Figure 4.11 shows the comparison of MATLAB Simulink simulation result and APS Technology experimental result for system with power 70%. Trend of the simulation curve and experiment curve of power 70% are similar and much accurate compare to curves of power 33%. The gradient of both curves are similar with similar mandrel is released time in experiment. Simulation curve is constant starting from around 2s, however it does not drop to zero due to the frictional force in the mandrel. From the experimental curve, it can be seen that displacement is fluctuating form 2s to 4s. However the degree of fluctuation is smaller compare to power 33%. This phenomenon could be contributed by noise and error when conducting the experiment. The deviation is very small comparing to simulation result thus making it within acceptable range of value.

#### **4.6 Time Shift**

During the experiment, it is discovered that the mandrel released time of simulation might be varies with the experimental data due to the accuracy of conducting experiment. For power 33%, range of time release is  $\pm 0.03$ s of the experimental value while for power 70%, the range of time release is  $\pm 0.05$ s. From the experimental data, the mandrel release time for power 33% is 0.091s, after using trial and error method, it is discovered that 0.07 is the best time to release the mandrel in the simulation. For power 70%, the release time of experiment is 0.055s. For the simulation, it is discovered that release time of 0.05s is the best time to fit the simulation and experimental curves.

## CHAPTER 5: CONCLUSION

From the Simulink simulation, it can be concluded that the higher the power of supply, the higher the damping coefficient. Besides that, vibration can be reduced effectively within a few seconds. Model that can reflect the experiment set up is constructed using MATLAB Simulink.

By using the constructed model, the behavior of vibration can be identified and estimated. Parameters such as mandrel released time and damping coefficient are studied. The main factors affecting the behavior of the system are force applied and damping coefficient. Furthermore, variables such as force applied, mass of mandrel, spring constant and damping coefficient can be adjusted easily in the software to study the effect and correlation of the variables on the displacement.

Future research can be done to study the effect of design of damper on vibration system. Designs of damper such gap of piston, piston diameter and piston length can be studied to obtain more accurate and complete results of the system.

## REFERENCE

1. Sapinski, B., Snamina, J. & Romaszko, M. (2012) The Influence of A Magnetic Field on Vibration Parameters of A Cantilever Beam Filled with MR Fluid. *Acta mechanica Et Automatic*, Vol.6 No.1
2. Walid H. E. (2002) Finite Element Analysis Based Modeling of Magneto Rheological Dampers.
3. Wassell et al. (2012) U.S. Patent No. 8,087,476 B2 System and Method for Damping Vibration in a Drill String Using a Magnetorheological Damper. *Washington, DC: U.S. Patent and Trademark*
4. Wassell M. et al. (2008) U.S. Patent No. US 2008/0315471 A1 System and Method for Damping Vibration in a Drill String. *Washington, DC: U.S. Patent and Trademark*
5. Wassell M. E., Cobern M. E., Saheta V., Purwanto A., Cepeda M. (2008) Active Vibration Damper Improves Performance and Reduces Drilling Costs. *World Oil*, pp. 108-111
6. Case D., Taheri B., Richer E. (2011) Multiphysics Modeling of Magnetorheological Dampers. Comsol Conference
7. Allotta B., Pugi L., Bartolini F., Design and Simulation of Magneto-rheological Dampers for Railway Applications
8. Ashfak A., Saheed A., Abdul Rasheed K. K., Abdul J. (2011) Design, Fabrication and Evaluation of MR Damper. *International Journal of Aerospace and Mechanical Engineering*
9. Kciuk S., Turczyn R., Kciuk M. (2010) Experimental and Numerical Studies of MR Damper with Prototype Magnetorheological Fluid. *Journal of Achievements in Materials and Manufacturing Engineering* Vol. 39 No. 1
10. Dubey H. K., Bhope D.V. (2012) Stress and Deflection Analysis of Belleville Spring. *IOSR Journal of Mechanical and Civil Engineering* Vol. 2 No. 5

11. Warren T. M., Oster J. H., Sinor L. A., Chen D.C.K. (1998) Shock Sub Performance Test. Paper IADC/SPE 39323
12. Parlak Z., Engin T., Calli I. (2012) Optimal Design of MR Damper via Finite Element Analyses of Fluid Dynamic and Magnetic Field. *Mechatronics* 22 pp. 890-903
13. Bajkowsi J. M. (2012) Design, Analysis and Performance Evaluation of the Liner, Magnetorheological Damper. *Acta Mechanical Et Automatica*, Vol. 6 No. 1
14. Sahin A., Engin T., Cesmecci S. (2010) Comparison of Some Existing Parametric Models for Magnetorheological Fluid Dampers. *Smart Materials and Structures*. IOP Publishing
15. Yalcintas M. (1999) Magnetorheological Fluid Based Torque Transmission Clutches. *The International Society of Offshore and Polar Engineers* Vol. IV
16. Wang J., Meng G. (2001) Magnetorheological Fluid Devices: Principles, Characteristics and Application in Mechanical Engineering. *Proceedings of the Institution of Mechanical Engineers* Vol. 215 Part L pp. 165-176
17. Fromm E., Kleiner W. (2003) Basic Calculation. *Handbook for Disc Springs*. Schnoor pp. 13-28

## APPENDIX

Table 2. Experimental and simulation result for power 33%

Experiment		Simulation	
Time (s)	Displacement (in)	Time (s)	Displacement (in)
0.0	3.030	0.000	3.0000
0.2	2.477	0.000	3.0000
0.3	1.942	0.000	3.0000
0.4	1.540	0.002	3.0000
0.5	1.262	0.008	3.0000
0.6	1.042	0.040	2.9994
0.7	0.865	0.070	2.9984
0.8	0.742	0.070	2.9984
0.9	0.647	0.070	2.9984
1.0	0.596	0.100	2.9758
1.1	0.568	0.131	2.9177
1.2	0.529	0.140	2.8941
1.3	0.529	0.187	2.7474
1.4	0.516	0.210	2.6625
1.5	0.477	0.280	2.3805
1.6	0.435	0.350	2.0911
1.7	0.418	0.420	1.8174
1.8	0.425	0.490	1.5703
1.9	0.425	0.560	1.3534
2.0	0.445	0.630	1.1668
2.1	0.428	0.700	1.0085
2.2	0.399	0.770	0.8755
2.3	0.369	0.840	0.7644
2.4	0.343	0.910	0.6723
2.5	0.343	0.980	0.5962
2.6	0.356	1.050	0.5335
2.7	0.376	1.120	0.4819
2.8	0.399	1.190	0.4396
2.9	0.366	1.260	0.4049
3.0	0.356	1.330	0.3765
3.1	0.296	1.400	0.3533
3.2	0.276	1.470	0.3343
3.3	0.296	1.540	0.3188
3.4	0.293	1.610	0.3061

3.5	0.329	1.680	0.2958
3.6	0.352	1.750	0.2874
3.7	0.359	1.820	0.2805
3.8	0.343	1.890	0.2748
3.9	0.329	1.960	0.2703
4.0	0.296	2.030	0.2665
		2.100	0.2635
		2.170	0.2610
		2.240	0.2590
		2.310	0.2573
		2.380	0.2560
		2.450	0.2549
		2.520	0.2540
		2.590	0.2532
		2.660	0.2526
		2.730	0.2521
		2.800	0.2517
		2.870	0.2514
		2.940	0.2512
		3.010	0.2509
		3.080	0.2508
		3.150	0.2506
		3.220	0.2505
		3.290	0.2504
		3.360	0.2503
		3.430	0.2503
		3.500	0.2502
		3.570	0.2502
		3.640	0.2501
		3.710	0.2501
		3.780	0.2501
		3.850	0.2501
		3.920	0.2501
		3.990	0.2500
		4.000	0.2500

Table 3. Experimental and simulation result for power 70%

Experiment		Simulation	
Time (s)	Displacement (in)	Time (s)	Displacement (in)
0.0	2.972	0.000	3.0000
0.1	2.877	0.000	3.0000
0.2	2.477	0.000	3.0000
0.3	2.105	0.002	3.0000
0.4	1.790	0.008	3.0000
0.5	1.499	0.040	2.9995
0.6	1.277	0.050	2.9992
0.7	1.113	0.050	2.9992
0.8	1.011	0.050	2.9992
0.9	0.915	0.060	2.9964
1.0	0.852	0.071	2.9889
1.1	0.777	0.091	2.9620
1.2	0.717	0.100	2.9463
1.3	0.644	0.144	2.8395
1.4	0.628	0.150	2.8216
1.5	0.609	0.181	2.7245
1.6	0.561	0.200	2.6586
1.7	0.561	0.250	2.4788
1.8	0.564	0.300	2.2954
1.9	0.542	0.350	2.1167
2.0	0.535	0.400	1.9473
2.1	0.503	0.450	1.7897
2.2	0.471	0.500	1.6448
2.3	0.480	0.550	1.5129
2.4	0.490	0.600	1.3935
2.5	0.487	0.650	1.2859
2.6	0.519	0.700	1.1894
2.7	0.487	0.750	1.1029
2.8	0.474	0.800	1.0256
2.9	0.431	0.850	0.9566
3.0	0.441	0.900	0.8951
3.1	0.454	0.950	0.8403
3.2	0.454	1.000	0.7915
3.3	0.474	1.050	0.7481
3.4	0.464	1.100	0.7095
3.5	0.451	1.150	0.6751

3.6	0.422	1.200	0.6445
3.7	0.402	1.250	0.6174
3.8	0.412	1.300	0.5932
3.9	0.445	1.350	0.5717
4.0	0.431	1.400	0.5526
		1.450	0.5357
		1.500	0.5206
		1.550	0.5072
		1.600	0.4953
		1.650	0.4847
		1.700	0.4752
		1.750	0.4669
		1.800	0.4594
		1.850	0.4528
		1.900	0.4470
		1.950	0.4417
		2.000	0.4371
		2.050	0.4330
		2.100	0.4293
		2.150	0.4260
		2.200	0.4231
		2.250	0.4206
		2.300	0.4183
		2.350	0.4163
		2.400	0.4144
		2.450	0.4128
		2.500	0.4114
		2.550	0.4101
		2.600	0.4090
		2.650	0.4080
		2.700	0.4071
		2.750	0.4063
		2.800	0.4056
		2.850	0.4050
		2.900	0.4044
		2.950	0.4039
		3.000	0.4035
		3.050	0.4031
		3.100	0.4028
		3.150	0.4025
		3.200	0.4022

		3.250	0.4019
		3.300	0.4017
		3.350	0.4015
		3.400	0.4014
		3.450	0.4012
		3.500	0.4011
		3.550	0.4010
		3.600	0.4009
		3.650	0.4008
		3.700	0.4007
		3.750	0.4006
		3.800	0.4005
		3.850	0.4005
		3.900	0.4004
		3.950	0.4004
		4.000	0.4003